Energy & Environmental Science

ANALYSIS

View Article Online
View Journal | View Issue

Cite this: *Energy Environ. Sci.*, 2015, **8**, 3069

Design guidelines for concentrated photo-electrochemical water splitting devices based on energy and greenhouse gas yield ratios†

Mikaël Dumortier and Sophia Haussener*

Received 23rd April 2015,
Accepted 10th August 2015

DOI: 10.1039/c5ee01269d

www.rsc.org/ees

Solar irradiation concentration is considered a viable strategy for reducing the energy and financial investment of photo-electrochemical hydrogen generation. We quantified and compared the sustainability benefit of this approach to non-concentrating and conventional approaches using life cycle assessment coupled to device performance modeling. We formulated design guidelines to reduce the environmental impact of a device. Model devices were composed of a concentrator module (with tracking, supporting, and framing components), photoabsorbers, membrane-separated electrocatalysts, and a cooling circuit. We selected eight concentrator types covering five concentrating technologies. For each device we studied the effect of the irradiation concentration ratio, electrode to photoabsorber area ratio, manufacturing requirements, incoming irradiance, and efficiency of components on sustainability utilizing two indices: (i) the energy yield ratio, and (ii) the greenhouse gas yield ratio. Both indices combine the performance of the system and its environmental impact. Two design guidelines were formulated based on the analysis: (i) any concentration-stable photoabsorber and electrocatalyst are equally feasible at concentrations larger than 55, as their performance prevails over their energy demand, and (ii) the system needs to be designed at an optimum concentration which depends on: performance, the relative surfaces of the photoabsorber and electrode, and irradiance. This study quantified and confirmed that concentrating solar irradiation has a beneficial effect on sustainability, energy yield, and greenhouse gas emissions compared to non-concentrated approaches. This was true for all concentrating technologies investigated. Consequently, this study provides an eco-performance-based rationale to further pursue the research and development of concentrated photo-electrochemical devices.

Broader context

Solar energy is the most abundant energy source but it is distributed and intermittent requiring its conversion and storage for meaningful use. Photoelectrochemical (PEC) conversion approaches provide a practical and impactful storage approach through the development of devices, which efficiently and continuously produce low cost hydrogen for several years. A fundamental requirement for any novel technology is its sustainability, which can be assessed by analysis of greenhouse gas emissions and energy requirements during all phases of its lifetime. Recent research on these devices focused not only on material selection for photoabsorbers and electrocatalysts, but also on their design. Concentrated solar irradiation has been suggested as an approach to reduce the cost of PEC devices as it replaces a large fraction of expensive materials by less costly collection and concentrating components. However, this approach needs to ensure that the beneficial effects are not overshadowed by additional energy requirements and emissions, and potential efficiency reduction. This article examines the effects of design, material selection, and operating conditions of concentrating PEC devices on performance and environmental indicators including: hydrogen production, cumulative energy demand, and greenhouse gas emission, in order to quantify the potential environmental and sustainable benefit of hydrogen generation by concentrated PEC conversion.

1 Introduction

The production of hydrogen by solar-driven electrolysis of water offers a direct pathway for the conversion and storage of solar energy into an energy-dense and transportable fuel. Such systems obtain their functionality by a combination of photo-active materials for charge generation and separation, and electrocatalytic materials for electrochemical reactions. Concentrating solar irradiation provides a pathway to address the cost issue of such devices using cheaper materials for radiation collection and redirection, together with a reduced area in the focal point where expensive and processing-intense materials

Laboratory of Renewable Energy Science and Engineering, EPFL, 1015 Lausanne, Switzerland. E-mail: sophia.haussener@epfl.ch; Tel: +41 21 693 3878

† Electronic supplementary information (ESI) available. See DOI: 10.1039/c5ee01269d

are required to be used.[1] Concentrated photovoltaic electrolyzers (CPVEs) are relatively novel and little knowledge is available regarding their performance and environmental impact. Peharz *et al.*[2] and Rau *et al.*[3] experimentally investigated a CPVE using a GaInP/GaInAs photoabsorber, and a Pt/Ir-based polymer electrolyte membrane electrolyzer. They demonstrated 18% and 16% solar-to-hydrogen efficiency and stable performance for up to 2 and 3 hours, respectively. Conceptual designs of integrated CPVEs have also been proposed[4–7] and design guidelines based on performance modeling have been provided.[6–8] Device performance decreased for concentrated irradiation due to increased current densities and corresponding increases in overpotentials, the appearance of mass transport limitations, and the decreased PV performance due to increased temperatures. These effects could be limited by appropriate dimensional and material choices. Nevertheless, holistic design guidelines are required to understand and quantify the benefit of concentrated devices. Such approaches consider efficiency but also economic and environmental impacts. Especially, characterization of the latter *e.g.* by quantifying specific greenhouse gas (GHG) emissions and the energy demand to manufacture and operate such a device are required in order to claim sustainability and to understand if and under which circumstances concentration can have an overall beneficial effect.

Life cycle analysis (LCA) can be used to characterize and quantify the environmental impacts of a device or a process throughout its life cycle. Few LCAs have been performed on solar driven electrolysis. Zhai *et al.*[9] published the first LCA of a photoelectrochemical (PEC) device and used the net primary energy requirement as the output index. Their analysis focused on the energy requirements for the fabrication of the cell assuming different combinations of materials and assessing the unknown energy requirements using a thermodynamic model. They observed that the energy required for the manufacturing of photoelectrodes was about two orders of magnitude larger than the energy required for procuring the photoelectrode materials. They also found that PEC device efficiencies and longevities larger than 5% and 5 years, respectively, are needed to ensure that the device produces more energy during its lifetime than consumed during manufacture and operation. Sathre *et al.*[10] extended the study, reporting the energy payback time (EPBT) and the energy return of investment (EROI) of a hypothetical 180 km^2 PEC hydrogen production facility with an energy output equivalent to 1 GW. The reported EPBT and EROI – 8.1 years and 1.7 – included the effect of decommissioning and balance of systems, *i.e.* structural supports, manifolds and pipes, pumps, compressors, storage tanks, pipelines, roads and monitoring systems. Their analysis identified the replacement of the PEC panels, the materials for the fabrication of the facility, and the compression of gases as the most energy-intense stages. A sensitivity analysis showed that the solar-to-hydrogen (STH) efficiency and the longevity of the panels were the most influential on EROI and EPBT. It is unclear if concentrated PEC (CPEC) devices and integrated CPVEs follow similar design guidelines, showing the same sensitivities, or if concentrations can reduce the environmental impact overall compared to un-concentrated PEC devices and integrated PVEs.

This study provides guidelines for CPEC and CPVE using coupled technical and environmental performance indicators. We conducted a LCA of integrated CPVEs to compare, guide, and optimize the design, performance, energy requirements, and GHG emissions. We studied classical solar concentration systems requiring tracking (parabolic trough collectors, concave mirrors, solar towers, and Fresnel lens concentrators), as well as a novel self-tracking wave-guide concentrator[11] and non-concentrating (integrated) PVE and PEC systems.

2 Methodology and system definition

2.1 Definition of the system and its boundaries

We followed the LCA methodology defined by the ISO standard 14040.[12] The operation of CPVEs is depicted in Fig. 1. Solar radiation is incident on a concentrator device, concentrating the radiation (characterized by its concentration factor C) and providing it to a photoabsorber, *e.g.* an integrated photovoltaic

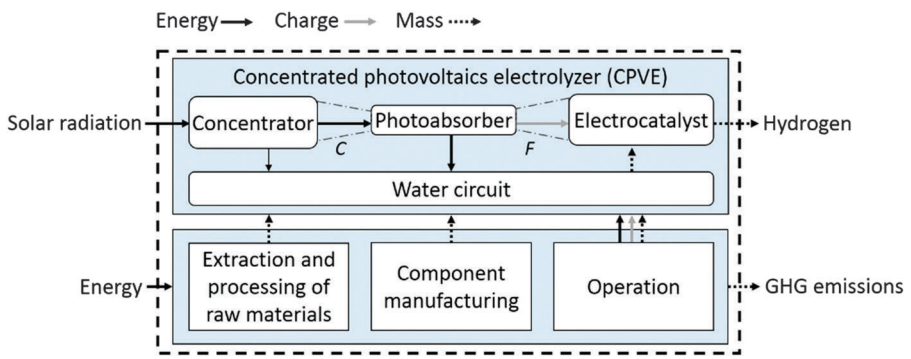

Fig. 1 System boundary and operating principle of the CPVE device, incorporating a concentrator, a photoabsorber (*e.g.* PV cell), separated electrocatalysts (*e.g.* PEMEC), and channels. The arrows follow the energy, charge, and mass transfer in the system. The thin arrow indicates that only the self-tracking wave-guide concentrator exchanges heat with the water circuit.[11] The area fraction between the solar concentrator and the photoabsorber is related to the irradiation concentration, C, ($C \geq 1$), and the area fraction between the photoabsorber and the projected electrocatalyst areas is related to the current concentration, F ($0 < F < \infty$).

(PV) cell. The generated charge pairs in the photoabsorber are separated and transported to an electrocatalyst driving the water electrolysis by separate water oxidation and proton reduction reactions. The electrocatalyst and the separator operating at near room temperature are grouped and encapsulated into a proton exchange membrane electrolysis cell (PEMEC). The current concentration between the photoabsorber and electrocatalysts is possible and characterized by a factor F representing the ratio between the projected electrode area and the photoabsorber area. The PV cell and PEMEC have the same areas and current densities if they are closely integrated, $A_{PEMEC}/A_{PV} = F = 1$, otherwise $F \neq 1$ (can be smaller or larger than 1) and the current densities in the PV and PEMEC differ.[13] In non-concentrating devices, the radiation of the sun is directly captured by the photoabsorber.

The solar radiation is concentrated by line-focusing (parabolic trough and linear Fresnel) and point-focusing (dish, point-focusing Fresnel, and solar tower) optical devices. These technologies require solar tracking for increased performance as the acceptance angle decreases with concentration. The concentrator module is considered to be composed of a tracking system including the metallic support of the module, and a concentrator including lenses or mirrors and array supports for the PV cell. Recently, a self-tracking solar concentrator has been demonstrated[11] using a fused silica glass wave-guide incorporating a dichroic membrane and wax layer assembly performing the actuation of light rays through its heat-driven deformation. This dichroic membrane and its deformation ensures that solar radiation with higher frequencies is reflected at an appropriate angle so as to be guided by the waveguide and concentrated onto the PV cell. The concentrator temperature increases with the rejected heat of the wax layer and can be additionally cooled to ensure optimal performance. This closely integrated concentrator which requires no additional tracking is referred to as the SHINE design.

The concentrator provides radiation to the photoabsorber, which converts it to electrical energy. The photoabsorber is an integrated multi-junction PV cell providing sufficient voltage to perform water electrolysis in the PEMEC at the highest possible current density. The PEMEC is composed of a polymeric electrolyte separating the anodic and cathodic compartments, catalytic layers, gas diffusion layers and flow plates. The anodic and cathodic electrochemical reactions, resistive losses in the liquid and solid conductors, and mass transport limitations, also taking into account bubble transport, lead to potential losses in the PEMEC. These overpotentials are especially significant for CPVEs operating at current densities comparable to commercial electrolyzers.[14] When using concentrated irradiation, the rejected heat in the PV cell and the PEMEC leads to increased temperatures. The temperature has a contradicting effect on the performance of integrated PEC or PVE devices namely it supports transport phenomena and electrochemical reactions while reducing the performance of the PV cell mainly due to increased recombination of charge carrier pairs and, consequently, reduced open circuit voltage losses.[8] In order to manage the heat flow in a CPVE for optimized performance, cooling of the PV cell and preheating of the reactants are considered. A water channel removes the heat from the PV cell and increases its temperature to the operating temperature of the PEMEC (≈ 80 °C). The water mass flow rate must provide sufficient reactants to the electrochemical reaction while ensuring that the fluid is heated to the electrolysis temperature. For the self-tracking concentrator (the SHINE concentrator),[11] water cooling is also used within the concentrator to cool and gather the rejected heat from the wax-layer assembly.

Our LCA estimates the energy demand and GHG emissions of the physical system composed of the concentrator module (including support and tracking), the PV cell (low and high performing), the PEMEC (low and high performing), and cooling/preheating channels (see Fig. 1). It includes pre-production points (*e.g.* extraction and production of raw materials), fabrication of the components, system production, and operation (including replacement of components). The transportation and assembly phase of elements as well as the dismantling phase and recycling of materials are not considered in this LCA. The processing of hydrogen at the outlet of the PEMEC – compression, storage in solids, or liquefaction – is also not included, but the impact of this process on the functional units will be assessed.

2.2 Functional units

We considered two metrics: the energy yield ratio (EYR) and the greenhouse gas yield ratio (GYR). The energy investment of photovoltaic systems is traditionally assessed by the EPBT, *i.e.* the lifetime at which a system has produced as much energy as it needed during its life cycle.[15,16] The EROI is a dimensionless quantity comparing the usable energy the system returns during its lifetime to all the invested energy needed to make this energy usable, and it therefore includes the lifetime of the system.[10,17] Richards *et al.*[18] underlined the fact that neither the EPBT nor the EROI include the lifetimes of the different components of the system, and proposed the EYR, a variation of the EROI, defined as:

$$\mathrm{EYR} = \frac{\dot{m}_{\mathrm{H_2}} \cdot \mathrm{LHV}_{\mathrm{H_2}}}{\sum_{i=1}^{n} \frac{\mathrm{CEDA}_i A_i}{L_i} + P_{\mathrm{op}}}, \quad (1)$$

using the year-averaged produced mass flow rate of hydrogen in kg year^{-1}, $\dot{m}_{\mathrm{H_2}}$, the lower heating value of hydrogen, $\mathrm{LHV}_{\mathrm{H_2}}$ = 120.97 MJ kg^{-1}, the year-averaged operational power in MJ year^{-1}, P_{op}, and the cumulative energy demand per unit area (CEDA) in MJ m^{-2},the area in m^2, and the lifetime in years of the ith component, $\mathrm{CEDA}_i A_i$, and L_i, respectively. A high EYR attests high energy payback of a device while EYR < 1 shows its inability to produce more energy than required for its production and operation during its life cycle. $P_i = \mathrm{CEDA}_i A_i / L_i$ is the lifetime-averaged yearly power cost of a component, including its CEDA, area and lifetime. The power cost per unit area, $p_i = \mathrm{CEDA}_i / L_i$, is expressed in MJ year^{-1} m^{-2}. This intensive variable does not depend on the size of the device, and hence will be used whenever possible.

The atmospheric impact of the device is assessed by the GYR in kg_{H_2} $kg_{CO_2\text{-eq}}^{-1}$, defined as:

$$\mathrm{GYR} = \frac{\dot{m}_{H_2}}{\sum_{i=1}^{n} \frac{\mathrm{CEGA}_i A_i}{L_i} + G_{\mathrm{op}}}, \quad (2)$$

using the cumulative GHG emissions per area (CGEA) of the ith component in $kg_{CO_2\text{-eq}}$ m^{-2}, $CEGA_i$, and the year-averaged GHG emission rate during operation in $kg_{CO_2\text{-eq}}$ $year^{-1}$, G_{op}. $g_i = CEGA_i/L_i$ is called the GHG flow per unit area of the component in $kg_{CO_2\text{-eq}}$ m^{-2} $year^{-1}$.

3 Life cycle inventory

The LCA investigates the energy and GHG emission data for the mining, manufacturing, and tracking operation processes only, providing a straightforward comparison of the different approaches and designs. Transportation, assembly, maintenance, and recycling of the system were not considered as they depend heavily on the location.

3.1 Cumulative energy demand of concentrator modules

The concentrator module is composed of a concentrator – frame, lenses or mirrors – and a tracking unit, which also acts as a supporting structure. The cumulative energy demand (CED) of the system, the fraction of CED devoted to the manufacturing of the concentrator module, and the calculated CEDA of the concentrator and the tracking unit of already existing concentrating technologies are shown in Table 1.

Three commercial point-focusing Fresnel lens (FL) based CPV systems were considered: AMONIX 7700, FLATCON, and a CPV system studied by Nishimura *et al.* referred to as GOBI.[19–21] These systems consisted of Fresnel lenses arranged on a module mounted on a 2-axis (AMONIX 7700) or a 3-axis (GOBI) tracker, acting as a support structure. An LCA of the SolFocusGen1 CPV system was reported by der Minassians *et al.*[22] The concentrator module was made of an array of small concave mirrors (CMs) and the CED of the different concentrator components was assessed by power calculations from the machinery specifications and from the producer price *via* the economic input–output LCA method.[27] Caballero[23] reported the CED of the central tower concentrating system (CTS) Gemasolar, located in Southern Spain, and the CED of the parts of the parabolic trough (PT) system Valle 1, also located in Southern Spain. Krishnamurthy *et al.*[24] assessed the CEDA of the Eurotrough PT collectors. They assessed the CEDA based on the mass of the components and the energy embodiment of the corresponding materials. The energy demand for the trackers and the concentration of the PT and CTS was not separately specified and we therefore assumed a usual geometric concentration between 25 and 70 for the PT system, and a concentration of 1410 for the CTS.[28] For point focusing concentration technologies, the CEDA of the 2-axis or 3-axis tracker is usually of the same order of magnitude as the CEDA of the concentrator. Therefore, the CEDA of the PT tracker was estimated to be 50% of the CEDA of the concentrator as only one-axis tracking was required.

For non-concentrating (NC) devices, we used a lower CEDA, since tracker and concentrator modules were not required. Only the manufacturing energy of the aluminum frame – ranging between 0 MJ m^{-2}, for frameless laminate modules, and 400 MJ m^{-2}, for PV panels – and the manufacturing energy of the support structure were considered.[25,26,29] The calculation of the self-tracking SHINE concentrator's CEDA and CGEA were assessed in detail and are presented in the ESI.†

The tracking power, *i.e.* the power of the motors required to operate the tracker, was estimated to be 50 W with a 12 h daily working time (30.9 MJ m^{-2} $year^{-1}$) and was considered the default tracking power in our study.[19]

3.2 Cumulative energy demand of PV cells

We chose two characteristic PV cells spanning a range of PV devices working fairly well (Ga-based cells) and fairly poor (Si-based cells) under concentrated irradiation. The primary energy requirements for an a-Si/μc-Si/μc-Si multi-junction PV cell was reported by Kim and Fthenakis.[30] The boundaries of their systems included the extraction and processing of raw materials (including the chemicals needed for the deposition processes), film deposition, and module production and operation. Recycling and disposal were not considered. They estimated the CEDA of the cell for different layer thicknesses, deposition rates, and gas usage, between 950 MJ m^{-2} and 1510 MJ m^{-2} corresponding to a mean value of 1230 MJ m^{-2} ± 23%. They found that the main contributions to the CEDA of these cells came from the electricity demand for the manufacturing of the

Table 1 CED of the complete CPV system, aperture area, and CEDAs for the concentrator and tracking of several solar concentrating technologies

Name	C	CED (TJ) CPV system	Area (m^2)	Concentrator module CED fraction (%)	CEDA tracker (MJ m^{-2})	CEDA concentrator (MJ m^{-2})
FLATCON (FL)	500	80.3	25.6	60	1286[19]	596[19]
AMONIX 7700 (FL)	550	1664.7	267	50	1600[20]	1529[20]
GOBI (FL)	500	5.5	10.9	88	196[21]	245[21]
SolFocus Gen1 (CM)	500	51.2	9[a]	66	1507[22]	2261[a 22]
Gemasolar (ST)	1410	640.7 × 10^3	304 750	45	946[23]	
Eurotrough (PT)	25–70	—	—	—	550[b]	1089[24]
Valle 1 (PT)	25–70	2380.1	817	50	1460[23]	
Non-concentrating (NC)	1	—	—	—	65 (support structure only)	200 (frame only)[25,26]
SHINE (self-tracking)	Tunable	—	—	—	1637 + 1635/C	

[a] The area was estimated at 9 m^2 based on a photograph. [b] The CEDA of the one-axis tracker was estimated to be 50% of the CEDA of the concentrator.

back reflector (24%), the electricity demand for the plasma-enhanced chemical vapor deposition process used to deposit the silicon layers (28%), and module manufacturing (26%). Mohr *et al.*[31] estimated the CEDA of a thin film GaInP/GaAs multi-junction PV cell to be 8540 MJ m^{-2}, almost 7 times higher than the CEDA of the Si-based cells. This large CEDA resulted from the production of high quality single-crystal GaAs and Ge wafers required as a template for deposition.

3.3 Cumulative energy demand of the PEMEC

The CEDA of the PEMEC was estimated using the data of Pehnt[32] and the ecoinvent database.[33] The obtained CEDAs were 3083 MJ m^{-2} and 2812 MJ m^{-2}, respectively, with a mean value of 2948 MJ m^{-2}. In Pehnt's study, PEMEC stacks of 75 kW_{el} and 275 kW_{el} were composed of two sets of membrane electrode assemblies, each made of two platinum loaded electrodes (0.3 mg cm^{-2}), two gas diffusion layers and a trifluorostyrene polymer proton conducting membrane. These sets were encapsulated between two graphite flow field plates. Electrodes, graphite plates, and gas diffusion layer manufacturing required 44%, 38% and 12%, respectively, of the total CED. The variation of CED induced by a change of catalysts is less than 10% since platinum, one of the most expensive electrode catalysts,[34] accounted for about 10% of the total CED.

3.4 Cumulative energy demand of the water circuit

In classical CPV systems, the water consumption required to clean and cool concentrator modules is around 1 kg m^{-2} $year^{-1}$.[20,35] In PVE devices, water must additionally supply the electrochemical reaction with reactants and match the current supply. A GaInP/GaAs PV cell produces a current density of about 25 A m^{-2} for an average radiation of 1953 kW h m^{-2} (see the reference case presented below), resulting in a minimum water consumption requirement of 38.4 kg $year^{-1}$ m^{-2} per unit area of the PV cell. We assumed that twice as much water is required to avoid the dry out of the membrane. Since the produced current density varies linearly with concentration for these PV cell types as well as the geometrical ratio of PV to concentrator areas, the required flow rate of water is 76.8 kg $year^{-1}$ m^{-2} per unit area of the concentrator. The energy for producing distilled water was assessed experimentally to be 3.6 kJ kg^{-1} by Moore *et al.*,[36] resulting in a power cost of 0.15 MJ $year^{-1}$ m^{-2} for a unit area of concentrator for the distilled water supply of the device, which is negligible compared to the power cost of other components. Considering a 5 mm wide, 1 mm thick, and 0.5 m long fused quartz pipe for PV cooling, the calculation showed that the pump power and CEDA to manufacture the pipe system was negligible (less than 1% of the overall energy requirement for the device).

3.5 Cumulative GHG emissions

A summary of the estimated specific emissions is given in Table 2. The CGEA of the AMONIX 7700 tracker was 118 $kg_{CO_2\text{-eq}}$ m^{-2}, the CGEA of the concentrator was 97 $kg_{CO_2\text{-eq}}$ m^{-2}, accounting for 23.4% and 28.4% of the total cumulated GHG emissions of the CPV device.[20] For non-concentrating technologies, Alsema *et al.* reported that 6.1 $kg_{CO_2\text{-eq}}$ m^{-2} was released during the production of the array support and the frame.[26]

The GHG emissions for the PV cells used in the present study were estimated from the existing data on amorphous and crystalline Si cells. CGEAs of 176, 235 and 286 $kg_{CO_2\text{-eq}}$ m^{-2} have been reported for 270–300 μm thick ribbon-Si, multi-Si and mono-Si single junction cells, respectively.[15,26] The thickness of a-Si/μc-Si/μc-Si PV cells used in the current study was expected to be around 127–130 μm,[30] consequently CGEAs were estimated to be between 80 and 134 $kg_{CO_2\text{-eq}}$ m^{-2}. Mohr *et al.*[31,37] and Meijer *et al.*[38] assessed the environmental impact of GaInP/GaAs modules as comparable to 270 μm thick multi-Si modules.

We estimated the GHG emissions of the PEMEC (using Pt catalysts) from Pehnt[32] to be 190 $kg_{CO_2\text{-eq}}$ m^{-2} and the ecoinvent database[33] to be 222 $kg_{CO_2\text{-eq}}$ m^{-2}, using the same calculation process as that used for the CEDA. The CGEA of the copper pipes used in the SHINE concentrator was estimated to be 143 $kg_{CO_2\text{-eq}}$ m^{-2}.[33] The GHG emissions of the tracking were assessed using the average EU energy mix with 0.1 $kg_{CO_2\text{-eq}}$ MJ^{-1}.[39]

3.6 Lifetime and degradation rates

The lifetime and degradation rates used in this study are summarized in Table 3. The methodology guidelines for the LCAs of PV producing electricity published by the International Energy Agency have proposed a 30 year lifetime for the framing, supporting structure, and PV device.[40] This life expectancy was based on typical PV module warranties (25 years) plus an expected addition of five years beyond. The report proposed a linear degradation in PV efficiency reaching 80% of the initial efficiency at the end of a lifetime of 30 years (0.7% efficiency reduction per year) based on the measurements of Skoczek *et al.*[41] These data were for non-concentrating devices and we expected an increase of degradation with increasing solar concentration. Wu *et al.* estimated a voltage loss of 2 to 10 μV h^{-1} for the PEMEC under normal operating conditions based on durability testing data.[42] Assuming a maximum of 250 mV voltage degradation before exchanging the cell, we estimated the lifetime of the PEMEC to be 10 years, which was more conservative than the 15 years of lifetime estimated by the ecoinvent database and Carmo *et al.*[14]

4 Modeling

4.1 Characteristics of the multi-junction PV cell and the PEMEC

Cooper *et al.* have shown that the performance of a GaInP/GaAs/Ge cell is stable for concentrations ranging from

Table 2 Average CGEA of the different elements used in concentrated and non-concentrated solar powered electrolyzers

Component	CGEA ($kg_{CO_2\text{-eq}}$ m^{-2})
Tracker	118[20]
Concentrator	97[20]
PV: thin film a-Si/μc-Si/μc-Si	107[15,26,30]
PV: thin film GaAs and GaInP/GaAs	540[31,37,38]
PEMEC (Pt catalysts)	206[32,33]
Copper pipes (SHINE)	143[33]
Array support (non-concentrating)	6.1[26]

Table 3 Lifetime and degradation rates of device components

Component	Lifetime	Efficiency degradation
Concentrator, frame, tracker	30 years[40]	None
Water system	30 years[40]	None
PV	30 years[40,41]	0.7% year^{-1} (ref. 40 and 41)
PEMEC	10 years[42]	6 μV h^{-1} (ref. 42)

1 to 1000 suns (1 sun = 1 kW m^{-2}) with a fill factor of around 85%, close to an ideal behavior.[43] We assumed the same behavior for the GaInP/GaAs tandem cell (band gaps of 1.9 eV and 1.43 eV)[37] and estimated its current–voltage characteristics by the Shockley–Queisser limit.[44] The current-potential behavior of a-Si/μc-Si/μc-Si PV cells under concentrated sunlight was estimated by averaging experimentally measured short circuit currents, i_{sc}, and open circuit voltages, V_{oc}, under standard conditions,[45] and combining these values with an experimentally measured fill factor decrease with increasing concentration under standard conditions.[46] For both PV cells, the concentration-dependence of i_{sc} and V_{oc} was estimated neglecting the effect of series and shunt resistances:[47]

$$i_{sc}(C,\phi) = C\phi/\phi_0 i_{sc}(1,\phi_0) \quad (3)$$

$$V_{oc}(C,\phi) = V_{oc}(1,\phi_0) + \frac{RT}{F_F}\ln(C\phi/\phi_0) \quad (4)$$

ϕ_0 is the irradiation value at which the reference short circuit currents and open circuit voltage have been calculated or measured. The loss in efficiency of the PV cell at the end of its lifetime is 20%. This was implemented *via* a lifetime-averaged 10% reduction in the short circuit current.

The operating voltage is the sum of the thermodynamic equilibrium potential required for the electrolysis of water under standard conditions, V_0, and current-dependent overpotentials due to chemical reactions, η_{act}, mass and charge transport, η_{conc} and η_{ohm}:[48]

$$V = V_0 + \eta_{ohm} + \eta_{act} + \eta_{conc}, \quad (5)$$

The mass transfer overpotential, η_{conc}, includes solution concentration variations, and possible bubble transport effects that lead to a potential loss. η_{conc} was estimated using a phenomenological model proposed by Kim *et al.*[49] and fit experimental results given by Dedigama *et al.*[50]

The exchange current density required for the determination of η_{act} is characterized by the projected surface area but might include effects of porous, nanostructured electrodes. On the other hand, the electrode to photoabsorber cell area, F, is not meant to assess the influence of the electrode's nanostructuring on the electrochemical behavior of the PEMEC. These effects are not non-linear and involve complex phenomena that would require a lower scale model to be accurately assessed.

The potential loss of the PEMEC at the end of its lifetime is 0.250 V. An additional lifetime-averaged 0.125 V potential loss was therefore added to account for the degradation of the device. The produced hydrogen mass flow rate was calculated using Faraday's law assuming a faradaic efficiency of 100%, *i.e.* no current leakage or parasitic reactions are considered. Detailed information on these models is given in the ESI.†

4.2 Reference case

The parameter values for the reference case are shown in Table 4, along with the range considered for sensitivity analysis. The AM 1.5 spectrum distribution is used and is weighed with the 1953 kW h m^{-2} year^{-1} yearly averaged direct normal insolation of Sevilla in southern Spain. We studied the response of the device with irradiance ranging from 1 kW h m^{-2} year^{-1} to 11 963 kW h m^{-2} year^{-1} (AM0 spectrum irradiance) since the response of the device is not linear with irradiance and therefore an average value may not be a representative of device performance.

We assumed full tracking of the sun for concentrating devices. For non-concentrating devices, the absence of tracking was accounted for with a reduced efficiency (50%) calculated from the 57% theoretical gain resulting from actuation.[51] The absorbed radiation was weighted by the optical efficiency of the concentrator; here the optical efficiency of the FLATCON's

Table 4 Parameter values for the reference case and the sensitivity analysis for the CPVE using the reference concentrator module or the self-tracking SHINE concentrator

Parameter	Reference values	Parameter range
Reference concentrator module		
Irradiance, Φ	1953 kW h m^{-2} year^{-1} (Sevilla)	1–11 963 kW h m^{-2} year^{-1}
Electrode to PV cell area, F	1	0.1–10
Concentration, C	1	1–1000
CEDA of the concentrator module	1941 MJ m^{-2}	0–4200 MJ m^{-2}
CGEA of the concentrator module	215 kg_{CO_2eq} m^{-2}	0–300 kg_{CO_2eq} m^{-2}
Power cost of the tracking	30.9 MJ year^{-1} m^{-2}	—
Power cost for distilled water supply	0.15 MJ year^{-1} m^{-2}	—
Concentrator optical efficiency, η_0	85%	10–100%
Concentrator lifetime, L	30 years	—
Exchange current density, i_0	3×10^{-8} A cm^{-2} (anode) 1.4×10^{-3} A cm^{-2} (cathode)	10^{-12}–10^{-4} A cm^{-2} —
SHINE concentrator		
Concentrator optical efficiency, η_0	42%	—
Concentrator lifetime, L	10 years	10–30 years

concentrator – 85% – has been measured and was chosen as the most reliable and conservative value,[19] compared to the 93% efficiencies considered for the AMONIX 7700[20] and the SolFocusGen1[22] concentrators. The measured optical efficiency of the SHINE concentrator is 42%.[11] We set the operating temperature of the PEMEC to 80 °C and the temperature of the PV cells to 25 °C, the temperatures reported in the experiments and used to derive their opto-electrical behavior.[45,46] The reference concentrator lifetime was set to 30 years (for all components) and a CEDA value corresponding to the average of all the reported values, excluding the SHINE concentrator, was assumed. The electrode to PV cell area, F, was varied from 0.1 to 10 to symmetrically assess the effect of this parameter on the sustainability of the device. IrO_2 and Pt were selected as the best catalysts for the anode and the cathode, respectively.[52] The efficiency and lifetime of the self-tracking SHINE concentrator were examined to assess the best improvement pathways.

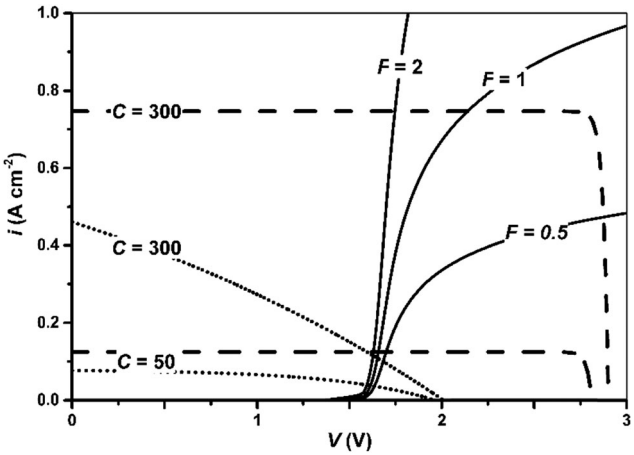

Fig. 2 Current density–voltage characteristics of the CPVE with GaInP/GaAs PV cells (dashed lines) or with a-Si/μc-Si/μc-Si PV cells (dotted lines) for C = 50 and 300 with the PEMEC at F = 0.5, 1, and 2 (solid lines). At large concentrations and small F values, mass transport limitations in the PEMEC decrease the operating current. The current density is given per PV area.

5 Results

5.1 Area fraction – C, F – variations and their influence on the EYR

C and F share the same geometrical meaning but show different performances and power cost behavior. C increases the available theoretical current density provided by the PV cell. Increasing F proportionally reduces the current density in the PEMEC, resulting in lower overpotentials and equal or higher operating currents. Typical current-potential characteristics of the PV and PEMEC are shown in Fig. 2, where the operating current density is indicated by the intersection between the PV power curves and the PEMEC load curves.

Decreasing F results in large current densities in the PEMEC, higher overpotentials at the same PV-current, and the appearance of mass transport limitations. Depending on the PV cell used, different C values are required to reach the same performance. For example, the operating current of a CPVE using a-Si/μc-Si/μc-Si PV cell and a CPVE using a GaInP/GaAs PV cell are about the same at C = 300 and C = 50, respectively, for F = 1, resulting from the low fill factor of the Si-based cell at high concentrations.

F and C also determine the area and mass of the components and therefore the power cost of the device. Fig. 3 shows the fraction of the concentrator module, PV cell, PEMEC, and tracking power on the power cost of the device per device area for the reference CPVE and the SHINE concentrator-based CPVE, both using GaInP/GaAs PV cells. Increasing C from 1 to 100 reduced the CPVE's power cost per unit device area from 674 to 96 MJ m^{-2} $year^{-1}$ for the reference concentrator module and from 906 to 164 MJ m^{-2} $year^{-1}$ for the SHINE concentrator module. The power cost of a device asymptotically decreased (for F = 1, and constant concentrator area) with increasing C due to the decreased required area of energy-intense components (PV cells and PEMECs). As a result, the PV cell and PEMEC contributed to less than 10% of the power cost for $C > 55$ in the reference concentrator and to less than 10% cost for $C > 30$ in the SHINE concentrator module. At high concentrations, the power cost fractions for the PV cell and the PEMEC approached zero, resulting in a constant of 67% and 33% power cost fraction for the concentrator and the tracking using the reference CPVE, and 100% for the concentrator using the CPVE based on the self-tracking SHINE concentrator.

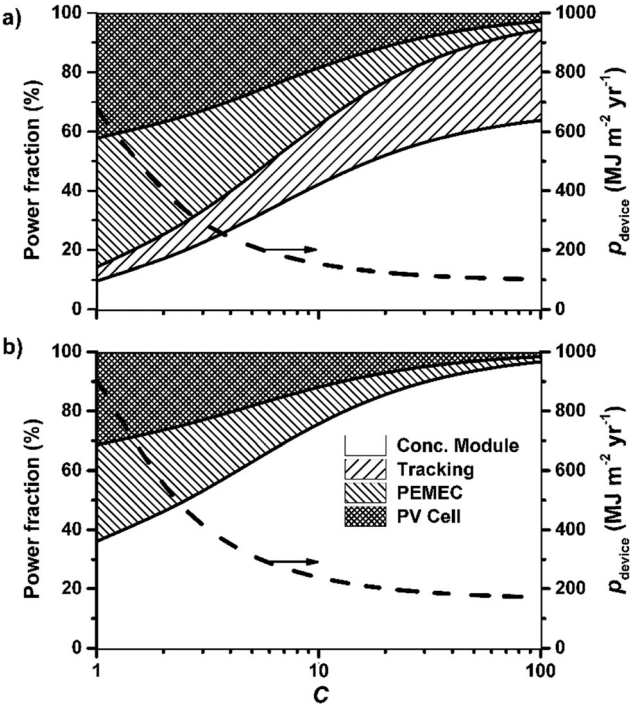

Fig. 3 Power cost fraction of the components of a CPVE device (left axis) and the total power cost of the device per unit device area (right axis) using a GaInP/GaAs PV cell as a function of C, using (a) the reference concentrator module, and (b) the SHINE concentrator. The power cost fraction of the PEMEC and PV cell are below 10% for $C > 55$ and 30 for the CPVE using the reference concentrator module and the SHINE concentrator, respectively.

While the power cost of the device decreased with increasing C, the hydrogen production rate (per area) remained constant with increasing C as i_{sc} is directly proportional to C. This trend was only observed up to an optimum concentration, C_{opt}, at which the increasing overpotentials push the PEMEC's i–V-curve away from the plateau region of the PV's i–V-curve leading to a significantly lower operating current. C_{opt} for the maximal EYR was reached at the best tradeoff between the reduced power cost and the reduced hydrogen production, as shown for the reference CPVE (see Fig. S1, ESI†).

The combined increase of C and F is beneficial for the EYR when using GaInP/GaAs PV cells, as depicted in Fig. 4a. This behavior results from the almost constant fill factor of the PV cell with increasing C, and from the reduction of the power cost fraction of the PEMEC and the PV cell with increasing C. The maximum EYR for the reference concentrator module EYR_{max} = 10.2 was obtained for C = 920 and F = 2.5 using GaInP/GaAs PV cells. At higher F values, the EYR decreases because power production remains at its maximum while the power cost of the PEMEC becomes more significant. The maximum EYR therefore results from a tradeoff between F, C, performance, and power cost of the device and its components. At large C and small F values, the mass transport limitations in the PEMEC lead to a sudden drop in the EYR. The device was not energetically sustainable (EYR < 1) for large F and small C values where the power cost of the PEMEC was too high, or for small F and large C values where the performance of the device was low, *i.e.* the operating current was small. For a-Si/μ-Si/μ-Si cells, the increased energy demand of the PEMEC with increasing F and the decreased fill factor with increasing C were not compensated by the beneficial effects of the reduced overpotentials in the PEMEC, see Fig. 4b. Consequently, the EYR was maximized at low F and C values, *i.e.* EYR_{max} = 3.84 at F = 0.108 and C = 5 for the reference concentrator module.

An ideal PEMEC with no transport limitations (η_{conc} = 0) and an ideal a-Si/μc-Si/μc-Si PV cell with a constant, concentration-independent fill factor (0.85) were tested as an optimistic case to account for the possible improvements of a-Si/μc-Si/μc-Si PV cells under concentrated radiation and for PEMEC designs that have succeeded in pushing the appearance of mass transport limitations to higher currents on a laboratory scale.[14,53] The maximum EYR of devices using GaAs/GaInP PV cells was not modified since i_{sc} does not depend on the PEMEC. For the same F, C_{opt} was higher (>1000) in this optimistic case and a higher EYR could be reached for lower F values as a result of the absence of mass transport overpotential. Devices using ideal a-Si/μc-Si/μc-Si PV cells showed similar trends compared to devices using GaAs/GaInP PV cells, but exhibited a lower EYR since i_{sc} and V_{oc} are lower for ideal Si-based PV cells. The maximum EYR reached by devices using ideal Si-based PV cells was 6.3 compared to 3.9 in the reference case using a realistic Si-based cell. The efficiency of the PV cell consequently influences C_{opt} and EYR_{max}, while the efficiency of the PEMEC influences C_{opt} only.

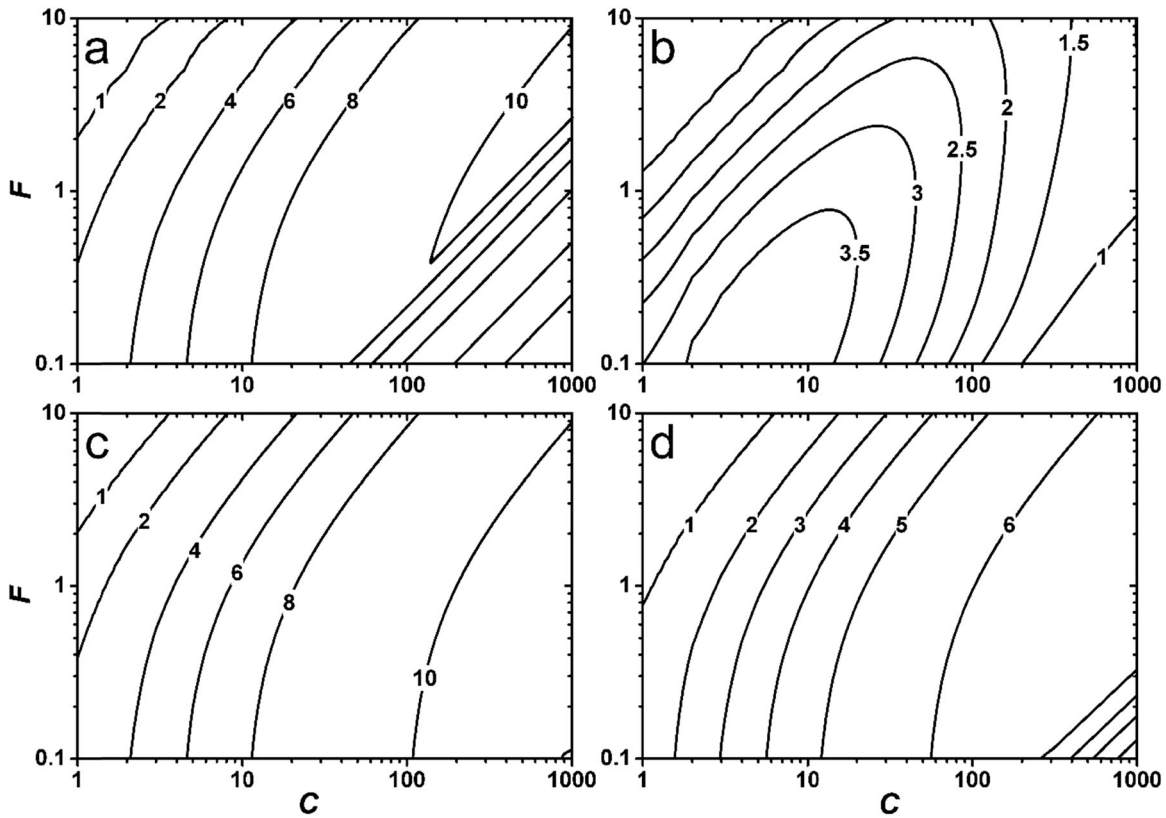

Fig. 4 EYR contours of the reference CPVE as a function of C and F using (a) GaInP/GaAs PV cells, and (b) a-Si/μc-Si/μc-Si PV cells, and of the ideal CPVE using GaInP/GaAs PV cells (c), and a-Si/μc-Si/μc-Si PV cells (d).

5.2 Concentrator technology choice's influence on EYR

The power cost of the concentrator module, $P_{\text{conc. mod}}$, is the major contributor to the overall power cost at high concentrations. Fig. 5 shows the combined effects of C and the concentrator module power cost per unit area, $p_{\text{conc. mod}}$, on the EYR for $F = 1$. C_{opt} is 360 for a CPVE device using a GaInP/GaAs PV cell with reference values, and varies between 10 and 20 for CPVE devices using an a-Si/μ-Si/μ-Si cell, since the power cost of the device is still decreasing with increasing concentration at such values of C (see Fig. 3). Despite a higher CEDA, using GaInP/GaAsPV cells resulted in a higher EYR, mostly because their fill factor is not changing with C and they provide larger i_{sc}. Using a-Si/μc-Si/μc-Si PV cells, parabolic troughs showed the best EYR (EYR = 3.8 at C = 70) while SolFocus Gen1 (EYR = 0.8) and AMONIX 7700 (EYR = 0.9) were not energetically sustainable. With Ga-based PV cells, CPVE devices using parabolic trough concentrator modules showed the highest EYR among the selected concentrator technologies (EYR = 11 for C = 70) and non-concentrating devices showed the lowest (EYR = 1.6). CPVE devices using the GOBI concentrator show even better performance (EYR = 16.22), but the CEDA of the GOBI concentrator module was unreasonably low (see Table 1). The operating concentrations of FL-based CPVEs were higher than C_{opt} for Si- and Ga-based PV cells. CPVEs with GaInP/GaAs PV cells and FLATCON, AMONIX 7700, or SolFocus-Gen1 concentrator modules have EYRs of 7.9, 5.5, and 4.8, respectively. The SHINE concentrator showed maximum EYR values of 6.7, 5.1, and 3 for 30, 20, and 10 lifetime years.

The dependence of C_{opt} on the optical efficiency is presented in Fig. S2 (ESI†) for the reference concentrator. The increase in η_0 led to a simultaneous increase of EYR and decrease of C_{opt}. For example, the optimum concentration of a 40% efficient concentrator was much higher (C = 780) than the optimum concentration of a 100% efficient concentrator (C = 310). Also, the same EYR = 4 was obtained at C = 29 for a 40%-efficient concentrator and at C = 3 for a 100%-efficient concentrator, indicating that the optical efficiency is a key parameter for the optimization of the device.

The EYR of a non-concentrating device is 6.3 and 2.4 times lower than the EYR obtained by the reference concentrating device for Ga-based and Si-based PV cells, respectively.

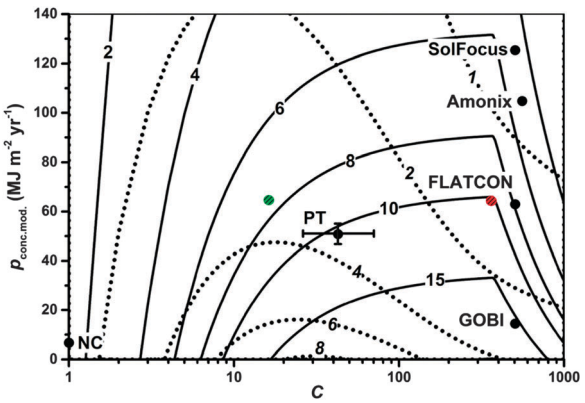

Fig. 5 EYR contours for the reference CPVE device as a function of concentration and the power cost of the concentrator module using a GaInP/GaAs PV cell (solid lines), and an a-Si/μc-Si/μc-Si PV cell (dotted lines). The various concentrator technologies investigated are indicated according to their respective power costs and concentration. The power cost of the non-concentrating (NC) devices was adapted to account for the absence of tracking. The reference concentrator is positioned at the optimum concentration for Ga-based cells C_{opt} = 360 with a red dot and at the optimum concentration for Si-based cells C_{opt} = 16 with a green dot.

5.3 Input power density influence on the EYR

Both C and Φ increase the effective power received by the PV cell but increasing C (at a constant A_{conc}) leads to a change in the PV cell and PEMEC cell areas leading to higher current densities. This increase in current density results in an earlier appearance of mass transport limitation for certain power inputs compared with a power increase achieved through enhanced irradiance. Fig. 6 compares the combined effect of realistic Φ and C on the EYR of the reference CPVE device using a GaInP/GaAs PV cell. The maximum EYR was reached for the largest possible irradiance at the corresponding C_{opt}. We observed that the same power input can result in different EYRs, depending on whether it is provided to the PV cell by concentrating the irradiance or by increasing the irradiance. For example, an EYR of 10.2 was obtained at a concentration of C = 360 in Tabernas, Spain, at C = 10 in Phoenix, USA, and at C = 1.6 under AM 1.5 irradiance. This highlights the importance of the location on the system performance and sustainability.

The nonlinear response of the device to irradiance called into question the validity of using a yearly averaged insolation to calculate the EYR. Table 5 shows the percentage error between EYR calculations using a daily, monthly, and yearly averaged irradiance compared to the EYR values of the reference case obtained with hourly averaged irradiance for C = 1, 50, 100, and 500. Daily, monthly, and yearly averaging included night periods, and therefore underestimated the value of instantaneous irradiation values that may bring the device to current density saturation. The different behavior of GaInP/GaAs PV cells below and above C_{opt} = 360 explained the high errors (more than 100%) for $C > 500$, while the smoother i–V curve of a-Si/μc-Si/μc-Si PV cells resulted in lower errors (less than 50%). C_{opt} changed with irradiance, and therefore with the time in the day indicating that a device with a fixed concentration will not continuously work at its optimum. This is in accordance with the observed efficiency variations during the day and year for an optimized device.[8] Ideally, the hourly averaged irradiance should be used if available but increases the calculation time by three orders of magnitude.

5.4 Catalysts' effect on the EYR

The oxygen evolution reaction shows low exchange current densities, i_0, and can be considered the limiting reaction. We varied i_0 of the oxygen evolution reaction between 10^{-12} and 10^{-4} A cm^{-2} in order to account for variations in the choice of the catalyst, its synthesis, changes in the operating temperature, or species concentration. Fig. 7 shows the EYR as a function of C and i_0 for the reference CPVE using a-Si/μc-Si/μc-Si PV cells. The device was sustainable for $1 < C < 540$ for $i_0 > 10^{-10}$ mA cm^{-2}.

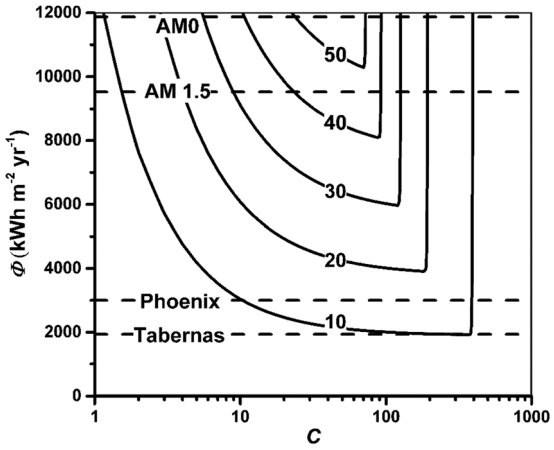

Fig. 6 EYR contour lines (solid lines) as a function of C and Φ for the reference CPVE with a GaInP/GaAs PV cell. Yearly averaged irradiance of Tabernas, Spain, and Phoenix, USA,[20] along with the reference irradiance AM1.5 and AM0 plotted as horizontal dashed lines.

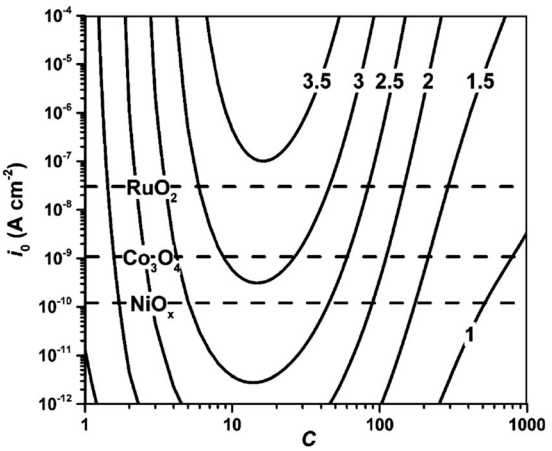

Fig. 7 EYR contour lines (solid lines) as a function of C and i_0 of the reference CPVE using a-Si/μc-Si/μc-Si PV cells. The dashed horizontal lines indicate anodic i_0 for common catalysts (NiO_x, Co_3O_4, RuO_2) under standard conditions.

Table 5 EYR calculated for concentrations 1, 50, 100 and 500, and the reference CPVE using the Ga-based or Si-based PVs with an hourly averaged irradiance. The labeled lines show the percentage error between instantaneous and daily, monthly, and yearly averaged irradiance for EYR calculations

PV cell	GaAs/GaInP				a-Si/μc-Si/μc-Si			
Concentration	1	50	100	500	1	50	100	500
EYR	1.46	9.2	9.7	7.8	1.2	2.9	2.3	1.3
Daily	2%	2%	14%	116%	3%	24%	31%	48%
Monthly	~0%	~0%	11%	119%	1%	22%	29%	46%
Yearly	~0%	~0%	12%	127%	1%	24%	31%	50%

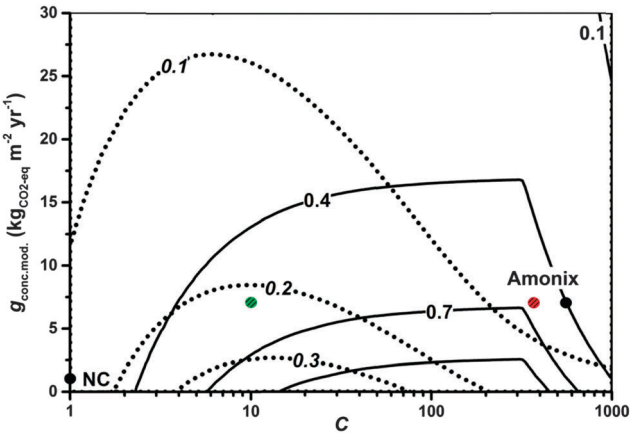

Fig. 8 GYR contour lines as a function of concentration and $g_{conc.\,mod}$ of the CPVE device using GaAs/GaInP PV cells (solid lines), and a-Si/μc-Si/μc-Si PV cells (dotted lines). $g_{conc.\,mod}$ of the non-concentrating (NC) devices were adapted to account for the absence of tracking and lower optical efficiency. The reference concentrator using Ga-based PV cells is positioned at C = 360 with a red dot and the reference concentrator using Si-based PV cells is positioned at C = 10 with a green dot.

The maximum EYR was obtained around C_{opt} = 16 and ranged from 2.9 to 3.4 for the exchange current densities of common oxygen evolution catalysts.[52] This indicates that the choice of C is more influential on the EYR than the choice of the catalyst. The effect of i_0 variation on the EYR for GaInP/GaAs PV cells was minimal (<1.7% for a given C), mostly because η_{act} didn't dominate the overpotentials in the operational space considered.

5.5 GYR for different concentrator's GHG

The maximum GYR of the reference CPVE is 0.58 kg_{H_2} $kg_{CO_2\text{-eq}}^{-1}$ at C = 360 and the GYR of the self-tracking SHINE concentrator is 0.46 kg_{H_2} $kg_{CO_2\text{-eq}}^{-1}$ at C = 620, both using GaAs/GaInP cells. The sensitivity analysis of the GYR showed similar trends as the sensitivity analysis of the EYR, given their close mathematical definition. Fig. 8 shows that the best GYR obtained using the non-concentrating devices (GYR = 0.2 kg_{H_2} $kg_{CO_2\text{-eq}}^{-1}$), the AMONIX 7700 concentrator module (GYR = 0.4 kg_{H_2} $kg_{CO_2\text{-eq}}^{-1}$ for Ga-based PV cells), and the SHINE concentrator (GYR = 0.46, 0.3 and 0.15 kg_{H_2} $kg_{CO_2\text{-eq}}^{-1}$ at C = 620 for 30, 20 and 10 years of lifetime, respectively, and Ga-based PV cells) never reached 1 for the reference case. This is valid for both Si- and Ga-based PV cells. This indicates that 1 kg of produced hydrogen will generate more than 1 kg of equivalent CO_2 GHG emissions. The GYR was lower for non-concentrating devices (0.13 kg_{H_2} $kg_{CO_2\text{-eq}}^{-1}$), the AMONIX 7700 concentrator module (0.07), and the SHINE concentrator (0.16 kg_{H_2} $kg_{CO_2\text{-eq}}^{-1}$ at C = 15 and L = 30 years) using Si-based PV cells than Ga-based PV cells because the lower hydrogen production of these cells did not compensate the reduction in GHG emissions.

The results were compared with other hydrogen processing routes for which GYR data were reported[54,55] and were adapted to our definition and system boundary which didn't account for hydrogen production and liquefaction. The comparison of the GYR of the various processes is shown in Table 6. The GYR for the non-concentrating PVE devices was comparable to what Koroneos *et al.*[54] obtained for the non-concentrating PVE (±15%). The GYR of our reference CPVE device (0.58 kg_{H_2} $kg_{CO_2\text{-eq}}^{-1}$) was 1.45 times larger than the GYR of the hydrogen production driven

Table 6 GYR for several hydrogen production technologies ranked according to the largest GYR

Rank	Technology for H_2 production	GYR (kg_{H_2} $kg_{CO_2\text{-eq}}^{-1}$)
1	Wind + electrolysis	1.18[54]
2	Hydropower + electrolysis	0.64[54]
3	CPVE	0.58 this study
4	AD[a] (100% conversion of methane)	0.47[55]
5	Thermal cracking	0.43[55]
6	Solar thermal + electrolysis	0.39[54]
7	AD[a] (50% conversion of methane)	0.38[55]
8	Biomass (gasification) + electrolysis	0.34[54]
9	SR[b] with CO_2 capturing and storage	0.29[55]
10	PV cells	0.17–0.2[54], this study
11	Natural gas SR[b]	0.08–0.1[54,55]

[a] AD: autocatalytic decomposition. [b] SR: steam reforming.

by solar thermal-generated electricity (0.39 kg_{H_2} $kg_{CO_2\text{-eq}}^{-1}$), 2 to 7.25 times larger than the GYR of steam reforming (SR) processes (0.08–0.29 kg_{H_2} $kg_{CO_2\text{-eq}}^{-1}$), 2.9 times larger than non-concentrating PVE devices (0.2 kg_{H_2} $kg_{CO_2\text{-eq}}^{-1}$), and 1.1 times lower than hydropower and electrolysis (0.64 kg_{H_2} $kg_{CO_2\text{-eq}}^{-1}$). The only hydrogen processing approach with predicted GYR > 1 kg_{H_2} $kg_{CO_2\text{-eq}}^{-1}$ is wind-powered electrolysis (GYR = 1.18 kg_{H_2} $kg_{CO_2\text{-eq}}^{-1}$).

5.6 Sensitivity analysis

Table 7 summarizes optimal EYR and GYR values obtained for reference or SHINE concentrator-based or non-concentrating CPVEs using either GaInP/GaAs or a-Si/μc-Si/μc-Si PV cells. All devices were energetically sustainable. Concentrating devices displayed a significantly better EYR than non-concentrating devices, *i.e.* for the same lifetime, 4.2–6.3 times higher for Ga-based cells and 1.6–2.4 times higher for Si-based PV cells. Similarly, the GYR of concentrating devices was 2.3–2.9 and 1.2–1.7 times higher than for non-concentrating devices for the same lifetime for Ga-based and Si-based PV cells, respectively. This confirms that using concentrated solar irradiation is meaningful in terms of sustainability.

Table 7 EYR and GYR for reference and self-tracking SHINE concentrators, with L = 10, 20 and 30 years and C_{opt} in brackets

	GaInP/GaAs PV cell		a-Si/μc-Si/μc-Si PV cell	
Concentrator	EYR	GYR	EYR	GYR
Non-concentrating	1.6	0.2	1.4	0.13
Reference	10.1 (360)	0.58 (360)	3.4 (16)	0.22 (10)
SHINE L = 10 years	3 (620)	0.15 (620)	1.1 (14)	0.06 (9)
L = 20 years	5.1 (620)	0.3 (620)	1.7 (17)	0.11 (12)
L = 30 years	6.7 (620)	0.46 (620)	2.2 (19)	0.16 (15)

The sensitivity of the maximum EYR and GYR, and C_{opt}, at which the product of EYR·GYR is maximized for the two photoabsorbers, was analyzed by varying the reference case parameters by +20% and is depicted in Table 8. Irradiance and optical efficiencies of the concentrator provided the highest increase in EYR and GYR (in a linear trend for both photoabsorbers) and the highest decrease in C_{opt} for GaInP/GaAs photoabsorbers. Reducing C_{opt} is desired as heat transfer and the management of hot spots becomes critical at high concentrations. A 20% increase of the CEDA and the CGEA of the concentrator module was followed by a negative variation of the EYR (−12% for GaInP/GaAs PV cells and −10% for a-Si/μc-Si/μc-Si photoabsorbers) and of the GYR (−9% for GaInP/GaAs and −8% for a-Si/μc-Si/μc-Si photoabsorbers). F impacted the value of C_{opt} in a significant way, *i.e.* a variation of F by 20% leads to an increase in C_{opt} by 22% for GaInP/GaAs PV cells and by 15% for a-Si/μc-Si/μc-Si PV cells. F has no significant effect on the maximum EYR and GYR since the energy fraction of the PEMEC and PV cells was already negligible. The variation of i_0 was too low to be significant (<0.01%). Storage of hydrogen was not considered in this study but will reduce the EYR of the device by 10%, as this is the fraction of the LHV_{H_2} required for liquefaction.[56]

6 Summary and conclusion

We conducted a life cycle assessment of an integrated solar powered electrolyzer device with a concentrated solar radiation input. The objective of solar irradiation concentration in solar

Table 8 Results of the sensitivity analysis indicating the variation in the maximum EYR, GYR, and the C_{opt} at the maximum product of EYR·GYR, for a parameter increase of +20% from their reference values. Red bars indicate a decrease, blue bars indicate an increase in the EYR, GYR, and C_{opt} with +20% of the input variable. Variations below 0.1% in absolute values are not shown

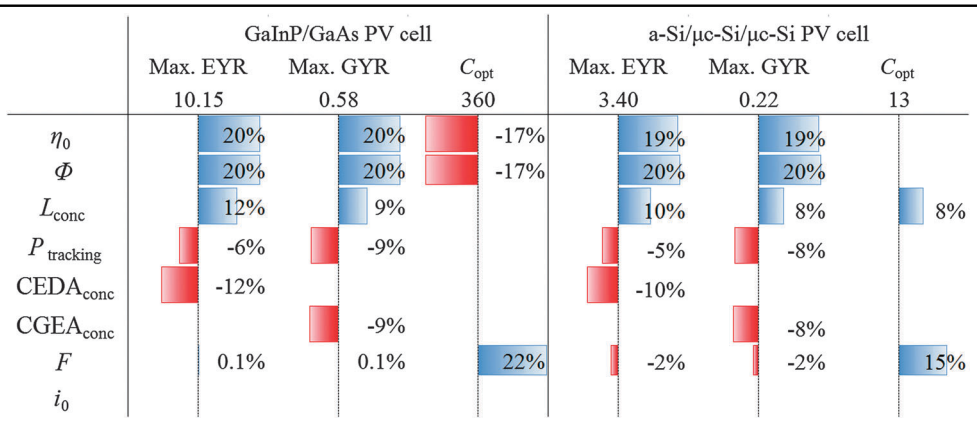

assisted hydrogen production is to reduce the weight and area of expensive, complex, and rare materials and device components, as these usually dominate the energy and financial costs of an overall device. A comparison and optimization of the performance, energy requirements, and greenhouse gas emissions between different concentrating technologies was conducted, and guidelines for a long-term energy strategy were formulated.

The device included a concentrator, a photoabsorber (photovoltaic cell), separated electrocatalysts (a proton exchange membrane electrolysis cell), and a cooling system. Commercial solar concentrating technologies – parabolic troughs, solar towers, and Fresnel lenses – were studied, along with a novel self-tracking wave-guide concentrator (called SHINE), as well as non-concentrating devices. These devices were compared using two eco-performance indicators: (i) the energy yield ratio (EYR), and (ii) the greenhouse gas yield ratio (GYR). The EYR and GYR account for the hydrogen production, the energy demand (or greenhouse gas emissions), the lifetime of the components, and the device operating power. The system boundary of this study included the extraction and processing of materials to manufacture the elements of the device as well as device operation. The energy requirement data were obtained from previous LCAs on concentrated solar technologies and PV cells and from the ecoinvent database. These data were coupled to a 0D performance model calibrated and fed with reported experimental data. The behavior of Si-based PV was fitted to a phenomenological performance model and the Shockley–Queisser limit was used to approximate the reported characteristics of Ga-based PV cells. An experimentally validated analytical model of the PEMEC was extended with a phenomenological mass transport term. Parameters such as irradiation fluxes, concentrator's optical efficiency, short circuit currents, open circuit voltages, electrical conductivities of the membrane, charge transfer coefficients and exchange current densities were taken from the reported experimental results.

Our study showed that the contribution of the PV cell and PEMEC components to the total power cost and green-house gas (GHG) emissions becomes less than 10% for concentrations above 55 for Ga-based and Si-based PV cells irrespective of the concentrating technology used. At high concentrations, the total energy cost of the device was mostly driven by the concentrator and by the power required for solar tracking. Therefore, the use of efficient absorbers and catalysts, which are generally the financial bottleneck of non-concentrated devices, can be chosen as long as they exhibit stability and large efficiency for hydrogen production at large irradiation concentrations. The power cost of the water circuit was less than 1% of the overall energy demand. This power cost could be reduced by adjusting the water demand to the required rate for electrolysis; however the energy gain would have to exceed the energy demand for any required auxiliary cooling system and heat exchanger. The operating power costs for tracking and water supply accounted for at least 20% of the total power cost. Potential self-tracking devices such as the novel SHINE concentrator reduced the tracking energy to zero.

The obtained values for the EYR were larger than 1 in most cases for a device using GaInP/GaAs PV cells attesting the sustainability of these devices. Devices using parabolic trough concentrating technologies showed the highest EYRs and GYRs. The EYR and GYR calculations of the novel, self-tracking SHINE concentrator predicted similar eco-performance to other high concentrating technologies (with $C > 500$, such as Fresnel lens based concentrating technologies), motivating further development of these novel concentrator types. These devices operated at the maximal EYR and GYR for an optimized concentration (C_{opt}), at which point the fill factor of the PV cell, the overpotentials in the PEMEC, and especially the mass transport limitations in the PEMEC start to dominate the behavior. This limit could be pushed towards higher concentrations by increasing the area of the PEMEC electrode (increasing F), resulting in a decrease of the overpotentials in the PEMEC. This increase in F is limited, as it simultaneously increases the PEMEC energy requirements. The optimum concentration depends on the material choices (mainly PV performance and concentrator optical efficiency), device design (F), and operating conditions (Φ), and is sensitive to the varying irradiation conditions (corresponding to spatial, daily, and seasonal irradiation variations), ideally requiring a concentrator with an adaptable concentration range. Such flexibility is not provided by current concentrating technologies and switching between concentrating technologies would be required. The concentration of the SHINE concentrator can be tailored to define a wide range of concentrations, making it particularly interesting for this application. The development of the self-tracking concentrator is able to follow the guidelines presented in this study additionally targeting materials that can further reduce the high CEDA of these devices.

The EYR and GYR of the device could be increased when utilizing the device in a location with larger irradiance than Sevilla (irradiance of 1953 kW h m^{-2} $year^{-1}$, chosen as a reference). Higher irradiance results in larger hydrogen production and lower optimum concentration values. We expect that the influence of the CO_2-intensity of the energy mix of the new location would lead to an insignificant increase in GYR. This study showed that the EYR and GYR remain quite stable (variations within $\pm$1.3% and $\pm$0.2% for the EYR and GYR) over a range of concentrations from 100 to 300 for GaAs/GaInP cells, contrary to Si-based PV cells (more than $\pm$7% for concentrations between 10 and 30). A concentration of 200 is recommended for Ga-based cells to account for the daily and seasonal irradiance variations. Furthermore, locations with higher irradiance are more beneficial for the sustainability of a device than locations with lower irradiance. Higher irradiation can compensate for lower concentration. Irradiance and optical efficiency of the concentrator were shown to be the most relevant parameters to improve the sustainability of the device since the variation of EYR and GYR is linear with these parameters in every configuration. The influence of exchange current density was negligible for devices with GaInP/GaAs PV cells with less than 1.7% variation for a given C for a range of values between 10^{-12} and 10^{-4} A cm^{-2}.

This study revealed that hydrogen processing by the CPVE outperforms, in terms of the GYR, the hydrogen production by

non-concentrating PV cells, as well as biomass gasification and natural gas steam reforming, while it unfavorably performs compared to hydrogen produced by hydro-powered electrolysis or wind energy-driven electrolysis. This study also revealed that the greenhouse gas emissions of hydrogen produced using an integrated concentrated PV electrolyzer device during its life cycle were up to seven times lower than that produced by hydrogen production through autocatalytic decomposition, non-concentrating PV electrolysis, or natural gas steam reforming. This study confirmed and quantified the beneficial effects of using irradiation concentration on sustainability, energy costs, and GHG emissions. The EYR increased from 1.6 to 6.3 times, and the GYR increased from 1.2 to 2.9 times, respectively, when using concentration compared to non-concentration devices, the exact value depending on the component choices.

This study confirmed that concentrating solar irradiation has a beneficial effect on the sustainability, energy yield, and greenhouse gas emission compared to non-concentrating approaches. This was true for all concentrating technologies investigated. Consequently, this study provides an eco-performance-based rationale to further pursue and intensify the research and development of concentrated photo-electrochemical devices.

Acknowledgements

This material is based upon work performed with the financial support of the Nano-Tera.ch support of the Nano-Tera.ch initiative, as part of the Solar Hydrogen Integrated Nano Electrolysis project (Grant # 530). The authors would also like to thank Volker Zagolla and Dr Didier Domine for fruitful discussion regarding the concentrator and PV performance.

References

1 B. A. Pinaud, J. D. Benck, L. C. Seitz, A. J. Forman, Z. Chen, T. G. Deutsch, B. D. James, K. N. Baum, G. N. Baum, S. Ardo, H. Wang, E. Miller and T. F. Jaramillo, *Energy Environ. Sci.*, 2013, **6**, 1983–2002.
2 G. Peharz, F. Dimroth and U. Wittstadt, *Int. J. Hydrogen Energy*, 2007, **32**, 3248–3252.
3 S. Rau, S. Vierrath, J. Ohlmann, A. Fallisch, D. Lackner, F. Dimroth and T. Smolinka, *Energy Technol.*, 2014, **2**, 43–53.
4 S. Tembhurne, M. Dumortier and S. Haussener, *Proceedings of the 15th International Heat Transfer Conference*, Kyoto, 2014.
5 J. Tuner, *Nat. Mater.*, 2008, **7**, 770–771.
6 B. Parkinson, *Sol. Cells*, 1982, **6**, 177–189.
7 Y. Chen, C. Xiang, S. Hu and N. S. Lewis, *J. Electrochem. Soc.*, 2014, **161**, F1101–F1110.
8 S. Haussener, S. Hu, C. Xiang, A. Z. Weber and N. S. Lewis, *Energy Environ. Sci.*, 2013, **6**, 3605–3618.
9 P. Zhai, S. Haussener, J. Ager, R. Sathre, K. Walczak, J. Greenblatt and T. McKone, *Energy Environ. Sci.*, 2013, **6**, 2380–2389.
10 R. Sathre, C. D. Scown, W. R. Morrow, J. C. Stevens, I. D. Sharp, J. W. Ager, K. Walczak, F. A. Houle and J. B. Greenblatt, *Energy Environ. Sci.*, 2014, **7**, 3264–3278.
11 V. Zagolla, E. Tremblay and C. Moser, *Opt. Express*, 2014, **22**, 13.
12 International Organisation for Standarization, ISO 14040 series, Envrionmental Management-Life Cycle Assessment, 2006.
13 C. Rodriguez and M. Modestino, *Energy Environ. Sci.*, 2014, **7**, 3828–3835.
14 M. Carmo, D. L. Fritz, J. Merge and D. Stolten, *Int. J. Hydrogen Energy*, 2013, **38**, 4901–4934.
15 V. M. Fthenakis, H. C. Kim and E. Alsema, *Environ. Sci. Technol.*, 2008, **42**, 2168–2174.
16 C. Reich-Weiser, D. A. Dornfeld and S. Horne, Proceedings of the 33rd IEEE Photovolatic Specialists Conference, San Diego, CA, USA, 2008.
17 D. Weißbach, G. Ruprecht, A. Huke, K. Czerski, S. Gottlieb and a. Hussein, *Energy*, 2013, **52**, 210–221.
18 B. S. Richards and M. E. Watt, *Renewable Sustainable Energy Rev.*, 2007, **11**, 162–172.
19 V. M. Fthenakis and H. C. Kim, *Prog. Photovoltaics*, 2013, **21**, 379–388.
20 G. Peharz, F. Dimroth and H. P. V System, *Prog. Photovolt.: Res. Appl.*, 2005, **13**, 627–634.
21 A. Nishimura, Y. Hayashi, K. Tanaka, M. Hirota, S. Kato, M. Ito, K. Araki and E. J. J. Hu, *Appl. Energy*, 2010, **87**, 2797–2807.
22 A. Der Minassians, R. Farshchi, J. Nelson, C. Reich-Weiser and T. Zhang, MSc thesis, U.C. Berkeley, 2006.
23 C. T. Hendrickson, L. B. Lave and H. S. Matthews, *Environmental Life Cycle Assessment of Goods and Services: An Input-Output Approach*, Routledge, London, 1st edn, 2006.
24 J. P. Caballero, BSc thesis, Universidad Carlos III de Madrid and Università degli studi de Perugia, 2012.
25 P. Krishnamurthy and R. Banerjee, *Lecture Notes in Information Technology*, 2012, vol. 9, pp. 509–514.
26 G. Augsburger, PhD thesis, Ecole Polytechnique Fédérale de Lausanne, 2013.
27 J. Peng, L. Lu and H. Yang, *Renewable Sustainable Energy Rev.*, 2013, **19**, 255–274.
28 E. A. Alsema and M. de Wild-scholten, Presented at 13th CIRP Intern. Conf. on Life Cycle Engineering, Leuven, 2006.
29 J. M. Mason, V. M. Fthenakis, T. Hansen and H. C. Kim, *Prog. Photovolt.: Res. Appl.*, 2006, **14**, 179–190.
30 H. C. Kim and V. M. Fthenakis, *Prog. Photovolt.: Res. Appl.*, 2011, **19**, 228–239.
31 N. Mohr, A. Meijer, M. A. J. Huijbregts and L. Reijnders, *Int. J. Life Cycle Assess.*, 2009, **14**, 225–235.
32 M. Pehnt, *Int. J. Hydrogen Energy*, 2001, **26**, 91–101.
33 *Ecoinvent V3.0*, Swiss Center for Life Cycle Inventories, 2013.
34 C. C. Rodriguez, M. M. A. Modestino, C. Moser and D. Psaltis, *Energy Environ. Sci.*, 2014, **7**, 3828–3835.
35 C. Turchi, M. Mehos, C. K. Ho and G. J. Kolb, Presented at SolarPACES 2010, Perpignan, 2010.
36 B. A. Moore, E. Martinson and D. Raviv, *Desalination*, 2008, **220**, 502–505.
37 N. J. Mohr, J. J. Schermer, M. A. J. Huijbregts, A. Meijer and L. Reijnders, *Prog. Photovolt.: Res. Appl.*, 2007, **15**, 163–179.

38 A. Meijer, M. A. J. Huijbregts, J. J. Schermer and L. Reijnders, *Prog. Photovolt.: Res. Appl.*, 2003, **11**, 275–287.
39 B. Metz, L. Kuijpers, S. Solomon, O. O. Andersen, S. Davidson, J. Pons, D. de Jager, T. Kestin, M. Manningl and L. Meyer, *Safeguarding the Ozone Layer and the Global Climate System: Issues Related to Hydrofluorocarbons and Perfluorocarbons*, Cambridge University Press, Cambridge, 2005.
40 V. Fthenakis, R. Frischknecht, M. Raugei, H. C. Kim, E. Alsema, M. Held and M. de Wild-Scholten, *Methodology Guidelines on Life Cycle Assessment of Photovoltaic Electricity*, International Energy Agency Report IEA-PVPS T12-03:2011, Upton, USA, 2011.
41 A. Skoczek, T. Sample and E. D. Dunlop, *Prog. Photovolt.: Res. Appl.*, 2009, 227–240.
42 J. Wu, X. Z. Yuan, J. J. Martin, H. Wang, J. Zhang, J. Shen, S. Wu and W. Merida, *J. Power Sources*, 2008, **184**, 104–119.
43 T. Cooper, M. Pravettoni, M. Cadruvi, G. Ambrosetti and A. Steinfeld, *Sol. Energy Mater. Sol. Cells*, 2013, **116**, 238–251.
44 W. Shockley and H. J. Queisser, *J. Appl. Phys.*, 1961, **32**, 510–519.
45 K. Söderström, G. Bugnon, R. Biron, C. Pahud, F. Meillaud, F.-J. Haug and C. Ballif, *J. Appl. Phys.*, 2012, **112**, 114503–114507.
46 L. M. van Dam and W. G. J. H. van Sark, *Proceedings of the 2011 MRS Spring Meeting*, San Francisco, 2011.
47 A. Luque and S. Hegedus, *Handbook of photovoltaic science and engineering*, Wiley, Hoboken, USA, 2003.
48 M. Ni, M. K. H. Leung and D. Y. C. Leung, *Int. J. Hydrogen Energy*, 2007, **32**, 2305–2313.
49 J. Kim, S. Lee, S. Srinivasan and C. E. Chamberlin, *J. Electrochem. Soc.*, 1995, **142**, 2670–2674.
50 I. Dedigama, K. Ayers, P. R. Shearing and D. J. L. Brett, *Int. J. Electrochem. Sci.*, 2014, **9**, 2662–2681.
51 H. Mousazadeh, A. Keyhani, A. Javadi, H. Mobli, K. Abrinia and A. Sharifi, *Renewable Sustainable Energy Rev.*, 2009, **13**, 1800–1818.
52 M. G. Walter, E. L. Warren, J. R. McKone, S. W. Boettcher, Q. Mi, E. A. Santori and N. S. Lewis, *Chem. Rev.*, 2010, **110**, 6446–6473.
53 S. A. Grigoriev, V. I. Porembsky and V. N. Fateev, *Int. J. Hydrogen Energy*, 2006, **31**, 171–175.
54 C. Koroneos, *Int. J. Hydrogen Energy*, 2004, **29**, 1443–1450.
55 J. Dufour, D. Serrano, J. Galvez, J. Moreno and C. Garcia, *Int. J. Hydrogen Energy*, 2009, **34**, 1370–1376.
56 M. T. Syed, S. A. Sherif, T. N. Veziroglu and J. W. Sheffield, *Int. J. Hydrogen Energy*, 1998, **23**, 565–576.

